THE JOURNAL OF BIOLOGICAL CHEMISTRY VOL. 289, NO. 19, pp. 13000–13009, May 9, 2014

SRA Gene Knockout Protects against Diet-induced Obesity and Improves Glucose Tolerance*

Received for publication, March 12, 2014 Published, JBC Papers in Press, March 27, 2014, DOI 10.1074/jbc.M114.564658

Shannon Liu[‡], Liang Sheng[§1], Hongzhi Miao[¶], Thomas L. Saunders[‖], Ormond A. MacDougald[‡§], Ronald J. Koenig[‡2], and Bin Xu[‡3]

From the [‡]Department of Internal Medicine, Division of Metabolism, Endocrinology and Diabetes, the Departments of [§]Molecular and Integrative Physiology and [¶]Pathology, and the [‖]Division of Molecular Medicine and Genetics, Transgenic Animal Model Core, University of Michigan Medical Center, Ann Arbor, Michigan 48109-5678

Background: The non-coding RNA, steroid receptor RNA activator (SRA), promotes adipocyte differentiation *in vitro*.
Results: SRA gene knock-out protects against obesity and improves glucose tolerance in mice fed a high fat diet.
Conclusion: SRA is an important regulator of adiposity in diet-induced obesity.
Significance: This is the first report that the *Sra1* gene plays an important role in adipose tissue biology *in vivo*.

We have recently shown that the non-coding RNA, steroid receptor RNA activator (SRA), functions as a transcriptional coactivator of PPARγ and promotes adipocyte differentiation *in vitro*. To assess SRA function *in vivo*, we have generated a whole mouse *Sra1* gene knock-out ($SRA^{-/-}$). Here, we show that the *Sra1* gene is an important regulator of adipose tissue mass and function. SRA is expressed at a higher level in adipose tissue than other organs in wild type mice. $SRA^{-/-}$ mice are resistant to high fat diet-induced obesity, with decreased fat mass and increased lean content. This lean phenotype of $SRA^{-/-}$ mice is associated with decreased expression of a subset of adipocyte marker genes and reduced plasma TNFα levels. The $SRA^{-/-}$ mice are more insulin sensitive, as evidenced by reduced fasting insulin, and lower blood glucoses in response to IP glucose and insulin. In addition, the livers of $SRA^{-/-}$ mice have fewer lipid droplets after high fat diet feeding, and the expression of lipogenesis-associated genes is decreased. To our knowledge, these data are the first to indicate a functional role for SRA in adipose tissue biology and glucose homeostasis *in vivo*.

Obesity results from an imbalance between energy intake and expenditure, in which the excess energy is stored as triglyceride in white adipose tissue (WAT)[4] with both increased fat cell size (hypertrophy) and number (hyperplasia) (1). Obesity induces a state of chronic, low grade inflammation in fat that is accompanied by the local secretion of cytokines and chemokines attenuating insulin action (2, 3). Recent genetic, cellular, and biochemical studies have identified a molecular network controlling the differentiation of WAT that involves a transcriptional cascade and epigenetic program beginning with CCAAT/enhancer-binding protein β (C/EBPβ) and δ (C/EBPδ) and the glucocorticoid receptor, which induce C/EBPα and peroxisome proliferator-activated receptor γ (PPARγ), the major transcriptional regulators of adipose differentiation (4–9). In addition, adipogenesis is regulated positively by a number of growth factors and hormones including insulin, insulin-like growth factor 1, and the bone morphogenetic proteins, and negatively by Wnt signaling (10, 11).

Long non-coding RNAs (lncRNAs) are non-coding transcripts that have recently emerged as important regulators in diverse biological processes (12, 13) including stem cell pluripotency, embryogenesis, and cellular differentiation. However, the function of lncRNAs in adipogenesis remains to be elucidated. The steroid receptor RNA activator (SRA) was initially characterized as a lncRNA that functions as an RNA coactivator to enhance steroid receptor-dependent gene expression (14). Our and other subsequent studies demonstrated that SRA also functions as an RNA coactivator for non-steroid nuclear receptors (15, 16) and the myogenic differentiation factor MyoD (17). The *Sra1* gene also produces an alternative transcript that encodes a protein denoted SRAP (18, 19), although the function of SRAP is largely unknown. Although SRA has been implicated to play a role in myogenesis (17, 20), steroidogenesis (21), breast tumorigenesis (22–24), and cardiomyopathy (25), the lack of a loss-of-function mouse model has limited our understanding of the *in vivo* biology of SRA.

We have recently shown that SRA promotes adipocyte differentiation and improves insulin-stimulated glucose uptake in adipocytes *in vitro* through multiple mechanisms, such as coactivating the transcriptional activity of PPARγ, promoting S-phase entry during mitotic clonal expansion, increasing phosphorylation of Akt/protein kinase B and forkhead box protein O1 (FOXO1) in response to insulin, and inhibiting expression of adipocyte-related inflammatory genes (26). To assess

* This work was supported, in whole or in part, by National Institutes of Health Grant R01DK62876 (to O. A. M.), a Pilot and Feasibility Grant (to B. X.) from the Michigan Diabetes Research Center, and NIH Grant P30DK020572 to the Chemistry Core of the Michigan Diabetes Research Center.
[1] Present address: Dept. of Pharmacology, School of Basic Medical Sciences, Nanjing Medical University, 140 Hanzhong Rd., Nanjing, Jiangsu 210029, China.
[2] To whom correspondence may be addressed. E-mail: rkoenig@umich.edu.
[3] To whom correspondence may be addressed: 5562 MSRBII, 1150 W. Medical Center Dr., Ann Arbor, MI 48109-5678. Tel.: 734-647-2883; Fax: 734-936-6684; E-mail: bxu@umich.edu.
[4] The abbreviations used are: WAT, white adipose tissue; C/EBP, CCAAT/enhancer-binding protein; PPARγ, peroxisome proliferator-activated receptor γ; SRA, steroid receptor RNA activator; LBM, lean body mass; HFD, high fat diet; qPCR, quantitative PCR; BAT, brown adipose tissue; TG, triglycerol; eWAT, epididymal white fat; DIO, diet-induced obesity; sWAT, subcutaneous white fat; SRC, steroid nuclear receptor coactivators; FM, fat mass; lncRNA, long non-coding RNA; SRAKO, *Sra1* gene knock-out.

SRA function *in vivo*, we have generated a whole mouse *Sra1* gene knock-out ($SRA^{-/-}$). In this study, we show that SRA is expressed at higher levels in adipose tissue than other organs. $SRA^{-/-}$ mice are resistant to diet-induced obesity with reduced fat content, decreased expression of subsets of adipocyte genes and inflammation genes, and improved insulin sensitivity. These data indicate an important role for SRA in adipose tissue biology *in vivo*.

EXPERIMENTAL PROCEDURES

Generation of Sra1 Gene Knock-out ($SRA^{-/-}$) Mice—Three mutant ES cell clones generated by gene targeting for mouse *Sra1* were obtained from the European Conditional Mouse Mutagenesis Program (EUCOMM). These targeted ES cell clones were generated in the C57BL/6N cell line JM8.N4 and are heterozygous for wild type *Sra1* and *Sra1*$^{tm1a(EUCOMM)Hmgu}$. For purposes of brevity, mice homozygous for the tm1a allele are referred to as $SRA^{-/-}$, and heterozygotes for wild type *Sra1* are referred to as $SRA^{+/-}$. The targeting cassette was inserted at position 36828917 of Chromosome 18 upstream of *Sra1* exon 3 (the targeting vector is shown in Fig. 2*A*). The cassette is composed of an FRT site followed by a *lacZ* sequence and a loxP site. The first loxP site is followed by a neomycin vector, a second FRT site and a second loxP site. A third loxP site is inserted downstream of the targeted exon 3. The critical exon 3 is thus flanked by loxP sites. Although a "conditional ready" (floxed) allele can be created by flp recombinase expression, in the present study the FRT-flanked cassette is left in place, resulting in a functional *Sra1* global knockout. Before injection, the ES cells were confirmed to contain the *Sra1* mutant gene by long range PCR. In addition, chromosome counting was performed to make sure that the receiving ES cells have at least 50% normal chromosome count. Finally, the ES cell clone HEPD0528_3_F03 with the best long range PCR signal and more than 80% normal chromosome count was microinjected into blastocysts of albino C57BL/6 mice (Jackson Laboratory Stock number 000058) to generate ES cell-mouse chimeras. Twenty-four male chimeras were bred with albino C57BL/6 female mice. Germ line transmission was evaluated by coat color and PCR. Genotyping was determined by LoxP3 site-spanning PCR (forward, 5′-TCCAAGTCTTTCCAGGAAAATG; reverse, 5′ ACAGAGCTTGTTTGTCTCTTC), *lacZ* PCR (forward, 5′ TTCACTGGCCGTCGTTTTACAACGTCGTGA; reverse, 5′ ATGTGAGCGAGTAACAACCCGTCGGATTCT), and long range PCR (primers used were as suggested by EUCOMM). Thus, we generated functional *Sra1* gene global knock-out mice (ablation of both SRA RNA and SRAP expression), denoted as heterozygous $SRA^{+/-}$ and homozygous $SRA^{-/-}$ (SRAKO) hereafter. The global SRAKO was further confirmed by RT-qPCR for SRA RNA and immunoblot for SRAP (antibody against SRAP was from Bethyl Laboratory, Inc., catalog number A300-742A). F0 germ-line transmitted males were backcrossed with C57BL/6J mice, the resulting F1 $SRA^{+/-}$ mice were intercrossed to derive $SRA^{+/+}$ (wild type, WT), $SRA^{+/-}$ and $SRA^{-/-}$ mice used for phenotype analysis and metabolic studies. Only male mice were studied for the phenotype of SRAKO. Genotyping was carried out by PCR analysis of genomic DNA extracted from the tails of progenies. Animals were housed on a 12-h light and 12-h dark cycle in the Unit for Laboratory Animal Medicine at the University of Michigan, with free access to water and a standard mouse diet; normal chow (9% fat; Lab diet) or a high fat diet (HFD) (60% fat; catalog number D12492, Research Diets, Inc., New Brunswick, NJ). All procedures were approved by the Institutional Animal Care and Use Committee of the University of Michigan.

Glucose and Insulin Tolerance Tests—For glucose tolerance tests, mice were subjected to fasting overnight (16 h) and D-glucose (2 g/kg of body weight) was injected intraperitoneally. Blood glucose was monitored at 0, 15, 30, 60, 120, and 180 min after glucose injection. For insulin tolerance tests, mice were subjected to fasting for 6 h and human insulin (1 IU/kg of body weight) was injected intraperitoneally. Blood glucose was monitored at 0, 15, 30, 60, and 120 min after insulin injection.

Food Intake—Food intake of normal chow was determined by measuring the remaining food weight weekly for singly housed mice for 6 weeks, and calculated from a 42-day average. At the end point of HFD feeding, the remaining weight of food provided was determined daily in metabolic cages for singly housed mice. Daily food consumption was calculated from a 3-day average.

Energy Expenditure and Respiratory Quotient—$SRA^{-/-}$ or WT littermate control mice post-HFD were placed in metabolic cages. The University of Michigan Metabolic Phenotyping Core measured oxygen consumption (VO_2), carbon dioxide production (VCO_2), and spontaneous motor activity during 3 consecutive days using the Comprehensive Laboratory Animal Monitoring System (Columbus Instruments), an integrated open-circuit calorimeter equipped with an optical beam activity monitoring system. Values presented are normalized to lean body mass (LBM) plus 20% fat mass (LBM + 0.2FM) to account for the fact that body composition differs between $SRA^{-/-}$ and WT mice (27). The respiratory quotient was calculated by dividing the carbon dioxide production by the oxygen consumption. We used the mean values for the light and dark cycles to analyze statistical significance.

Body Composition—Body fat, lean body mass, and fluid content in $SRA^{-/-}$ mice and WT littermate controls after HFD experiments were measured using nuclear magnetic resonance analysis in The University of Michigan Metabolic Phenotyping Core.

Histology—Tissues were fixed in 10% buffered formalin, and histology was assessed by hematoxylin and eosin (H&E) staining at the University of Michigan Cancer Center Research Histology Laboratory.

Gene Expression Analysis—Isolated mouse tissues were rinsed in phosphate-buffered saline (PBS), frozen in liquid nitrogen, and stored at −80 °C until extraction. Total RNAs from WAT, brown adipose tissue (BAT), liver and skeletal muscle were isolated using TRIzol reagent followed by treatment with DNase I (Qiagen). RT-qPCR analysis of gene expression was as described previously (21, 26). Primers are listed in Table 1. To determine whether SRA expression is induced by high fat diet feeding, samples of inguinal WAT from male C57BL/6J mice were provided by Dr. Cliff Rosen (Maine Medical Center Research Institute, Scarborough ME). The mice were fed standard chow diet or HFD *ad libitum* from 3 to 15 weeks of age. The

TABLE 1
Primers used in RT-qPCR for mRNA expression analyses

Gene name	NCBI Ref. Seq. #	Forward primer	Reverse primer
Sra1	NM_025291.3	GGCTGGAGGGAAGTTGTCAATAC	CCACTGGTGATGTAAAAGTTCTTG
Pparg	NM_001127330.1	GGAAAGACAACGGACAAATCAC	TACGGATCGAAACTGGCAC
Cebpa	NM_001287514.1	TGAACAAGAACAGCAACGAG	TCACTGGTCACCTCCAGCAC
Fabp4	NM_024406.2	TGGAAGCTTGTCTCCAGTGA	AATCCCCATTTACGCTGATG
Lipe	NM_001039507.2	GGCAAAGAAGGATCGAAGAAC	TGTGTCATCGTGCGTAAATC
Cd36	NM_001159555.1	GAACAGCAGCAAAATCAAGG	AAGACACAGTGTGGTCCTC
Pck1	NM_011044.2	TCGAAAGCAAGACAGTCATC	CAAAGTCCTCTTCCGACATC
Ppia	NM_008907.1	TCCAAAGACAGCAGAAAACTTTCG	TCTTCTTGCTGGTCTTGCCATTCC
Ccl2	NM_011333.3	AGATGATCCCAATGAGTAGGC	CACAGACCTCTCTCTTGAGC
Adipoq	NM_009605.4	AAGAAGGACAAGGCCGTTCTCTT	GTCATGGGTAGTTGCAGTCAGTT
Tnf	NM_001278601.1	CCACGCTCTTCTGTCTACTG	TCTGGGCCATAGAACTGATG
Il6	NM_031168.1	CAAGTCGGAGGCTTAATTACAC	TGCAAGTGCATCATCGTTG
Ncoa1	NM_010881.2	CATGCAGCCCCGGCAGACTC	GCATCAACTGCTGCTGCCCCT
Ncoa2	NM_001077695.1	AGCTGACAGCAGTCCCGTCCC	TGCTGCTGCCAATCATTCTGCTCT
Ncoa3	NM_008679.3	GAAGATGGCGGCGAGCGGATCA	CAGGAAGGGCAGGAAGAGCTTCG
Prdm16	NM_001177995.1	AGCCGGGAAGTCACAGGAGGAC	CATTGCATATGCCTCCGGGTATGG
Cidea	NM_007702.2	GCCCTCATCAGGCCCCTGACAT	ATCACCCCACGCCGGCTACT
Ucp1	NM_009463.3	GTACAGCGGTCTGCCTGCGG	TCCGAGAGAGGCAGGTGTTTCTCT
Cycs	NM_007808.4	CTCCACGGTCTGTTCGGGCG	TCCTCTCCCCAGGTGATGCCTTT
Cox8b	NM_007751.3	CCCTATCCTGCGGCTGCTCCA	AGCCTGCTCCACGGCGGA′AG
Ppara	NM_001113418.1	CATCGAGTGTCGAATATGTGG	CAGCTTCAGCCGAATAGTTC
Srebf1	NM_011480.3	GAGAACCTGACCCTACGAAG	TCATGCCCTCCATAGACAC
Scd1	NM_009127.4	GAAGTCCACGCTCGATCTCA	TGGAGATCTCTTGGAGCATGTG
G6pc	NM_008061.3	ACGCCCGTATTGGTGGGTCC	GCCAGAGGGACTTCCTGGTCCG
Slc2a2	NM_031197.2	CCCGTCCTACGGCTCTGGCA	GGCCCAAGGAAGTCCGCAATGT
Pgc1a	NM_008904.2	AGACACCGCACACACCGCAAT	TCATAGCTGTCGTACCTGGGCCT
Rplp0	NM_007475.5	ACCGCCTGGTTCTCCTATAAAAGGC	ACGATGTCACTCCAACGAGGACG
Tbp	NM_013684.3	GCACAGGAGCCAAGAGTGAA	TAGCTGGGAAGCCCAACTTC
Cd137	NM_001077508.1	CGTGCAGAACTCCTGTGATAAC	GTCCACCTATGCTGGAGAAGG
Bmp8b	NM_007559.4	CTATGCAGGCCCTGGTACATC	GTAGGCACACAGCACACCTT
Fndc5	NM_027402.3	TCTTCATGTGGGCAGGTGTTA	GGTTTCTGATGCGCTCTTGG
Tbx1	NM_001285472.1	CGCTACCGGTATGCTTTCCA	GTAGTGTACTCGGCCAGGTG
Tbx15	NM_009323.2	TGGCAGAAACAGAACTGGACT	CCTTGCTGCTTTTGCATGGT

mice became obese on the HFD with 40% body fat compared with 18% body fat with the normal chow diet, at which point inguinal WAT was isolated for RNA purification as described (28) and subjected to RT-qPCR.

Stromal Vascular Fraction and Adipocyte Isolation—We digested excised epididymal white adipose tissue (eWAT) from 8-week-old male C57BL/6J mice in PBS containing 1% bovine serum albumin (BSA) and 1 mg ml^{-1} of type II collagenase for 30 min at 37 °C with gentle agitation. The cell suspension was filtered through a 100-μm filter and then centrifuged at 700 × *g* for 5 min to separate floating adipocytes from the stromal vascular fraction pellet. Floating adipocytes were then washed twice with PBS containing 1% BSA. The pellets representing the stromal vascular fraction were collected after each wash.

Blood Chemistry Analysis—Blood samples collected from the tail vein were used to measure blood glucose by a OneTouch Ultra Glucometer. Plasma from mice fasted for 6 h was isolated from whole blood collected into heparinized tubes. Plasma insulin, leptin, TNFα, and IL6 concentrations were measured using luminex technology in a multianalyte panel plate purchased from Millipore in the Chemistry Laboratory of University of Michigan Diabetes Research Center. Plasma adiponectin levels were determined using a mouse adiponectin radioimmunoassay kit from Millipore (catalog number MADP-60HK). Serum triglyceride (TG) and serum and liver non-esterified fatty acid levels were measured using TG (Pointe Scientific Inc., catalog number T7532-120) and non-esterified fatty acid assay kits (Wako Pure Chemical Industries, Ltd.). Liver TG was extracted by chloroform:methanol, 2:1, evaporated to dryness, and hydrolyzed by KOH. After addition of $MgCl_2$, the glycerol liberated from TG was assayed by glycerol reagent (Sigma catalog number F6428) for TG determination.

In Vivo Analysis of Insulin-stimulated Phosphorylation of Akt in HFD-fed Mice—Mice after a 2-week HFD feeding were fasted 16 h, then injected with PBS or human insulin (3 units/kg of body weight) via the tail vein. Five minutes later, eWAT, liver, and gastrocnemius muscles were dissected, frozen in liquid nitrogen, and stored at −80 °C. Tissues were homogenized in ice-cold T-PER Tissue Protein extraction Reagent (Pierce number 78510) containing phosphatase inhibitor mixture (Thermo Scientific, catalog number 1862495) and protease inhibitor mixture (Roche Applied Science, catalog number 11836170001). The extracts were subjected to gel electrophoresis and immunoblotted with antibodies directed against Phospho-Akt (Ser-473) (catalog number 9271) or Akt (catalog number 9272) obtained from Cell Signaling Technology (Danvers, MA).

Statistical Analyses—All values are presented as the mean ± S.D. and were analyzed by two-tailed Student's *t* test. Statistical significance is defined as $p < 0.05$, and the term "trend" is used to describe comparisons for which $0.05 \leq p \leq 0.10$.

RESULTS

SRA Is Highly Expressed in Adipose Tissues—We have shown recently that SRA expression is induced during 3T3-L1 cell adipocyte differentiation *in vitro* (26). To study SRA function *in vivo*, we first examined the expression levels of SRA in several murine tissues, and showed that SRA is expressed at the highest levels in WAT, followed by BAT (Fig. 1*A*). Expression of SRA was significantly higher in the adipocyte fraction than in the stromal-vascular fraction of WAT from lean mice (Fig. 1*B*). In

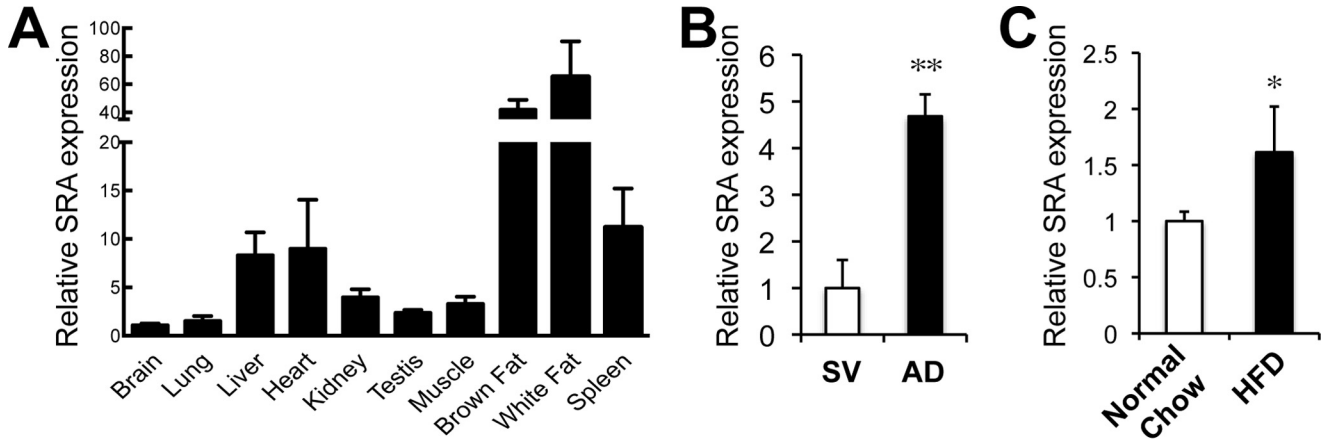

FIGURE 1. **SRA is highly expressed in adipose tissue *in vivo*.** *A*, tissue expression was analyzed by RT-qPCR for mouse SRA. Total RNA was isolated from each tissue of 9-week-old C57BL/6J mice. The locations of adipose depots analyzed were interscapular BAT and epididymal WAT. Data were normalized to peptidylprolyl isomerase A (*Ppia*) mRNA and expressed relative to levels in whole brain, $n = 6$. *B*, total RNA was isolated from the stromal-vascular fraction (*SV*) or adipocytes (*AD*) of epididymal WAT from 8-week-old male C57BL/6J mice. SRA RNA expression was determined by RT-qPCR. Expression of SRA was normalized to TATA box-binding protein (*Tbp*) because it is expressed at similar levels in both fractions, and relative to levels in the stromal-vascular fraction set at 1, $n = 10$. *C*, male C57BL/6J mice were fed normal chow or HFD from 3 to 15 weeks of age. Total RNA was then isolated from inguinal WAT. Expression of SRA was analyzed by RT-qPCR and normalized to *Ppia* mRNA. Data are expressed as fold-change relative to the SRA level of normal chow mice, $n = 4–5$ mice per group. Data are presented as mean ± S.D. Statistical significance in *B* and *C* was evaluated with Student's *t* test: **, $p < 0.01$; *, $p < 0.05$.

addition, SRA expression was significantly induced in WAT from HFD-induced obese mice compared with control mice fed normal chow (Fig. 1*C*). Consistent with our previous findings that SRA promotes adipogenesis in cell culture (26), these observations suggested that SRA may also play an important role in adipose tissue biology *in vivo*.

Generation of Sra1 Gene Knock-out (SRAKO) Mice—To directly investigate the role of SRA in adipose tissue *in vivo*, we have generated SRAKO mice and characterized them with respect to energy and glucose homeostasis. The targeting vector includes a *lacZ*/neo cassette with transcription termination signals flanked by FRT sites (Fig. 2*A*). The cassette was not excised, which is predicted to result in loss of SRA expression and hence a global functional gene knock-out (29).

Five males and four females of the F0 germline transmitted mice were obtained. After backcrossing with C57BL/6J mice, the resulting F1 heterozygous ($SRA^{+/-}$) mice were intercrossed to derive wild type control ($SRA^{+/+}$), heterozygous ($SRA^{+/-}$), and homozygous ($SRA^{-/-}$) mice, which were confirmed by PCR genotyping (Fig. 2*B*). The $SRA^{+/-}$ and $SRA^{-/-}$ mice appeared normal. The genotypes of 233 F1 pups obtained at weaning stage included 50 $SRA^{+/+}$, 120 $SRA^{+/-}$, and 63 $SRA^{-/-}$ mice, which nearly matched the expected 1:2:1 Mendelian ratio.

SRA RNA expression was assessed in WAT, BAT, liver, and skeletal muscle by RT-qPCR (Fig. 2*C*, *upper panel*). SRA RNA expression was reduced ~50% in $SRA^{+/-}$ mice and was absent in $SRA^{-/-}$ mice. Similar results were obtained for the SRA protein (SRAP), assessed by Western blot (Fig. 2*C*, *lower panel*). These results confirm successful knock-out of SRA and SRAP expression.

$SRA^{-/-}$ Mice Are Protected against Diet-induced Obesity (DIO) and Have Decreased Expression of Adipocyte Genes—The $SRA^{-/-}$ mice were without significant body weight changes at the age of weaning (3 weeks) and during postweaning 3–6 weeks when fed a normal chow diet (Fig. 3*A*). At age 6 weeks the $SRA^{-/-}$ and WT littermate control ($SRA^{+/+}$) mice were placed on a HFD. After 14 weeks on this diet, $SRA^{-/-}$ mice weighed 6 g less than the WT controls, indicating the $SRA^{-/-}$ mice are resistant to diet-induced obesity (Fig. 3*A*). Characterization of body composition revealed that the differences in total body weight were due to reduced % fat mass, with increased % lean mass in $SRA^{-/-}$ mice (Fig. 3*B*). As expected from these results, the $SRA^{-/-}$ mice had reduced epididymal white fat (eWAT) and subcutaneous white fat (sWAT) mass (Fig. 3*C*). Interestingly, $SRA^{-/-}$ mice also had reduced liver mass (Fig. 3*D*). The reduced fat mass in $SRA^{-/-}$ mice was associated with small adipocytes in eWAT compared with WT mice (Fig. 3*E*).

We have recently shown that SRA promotes adipocyte differentiation *in vitro* at least in part through coactivating the transcriptional activity of PPARγ, the master regulator of adipogenesis (26). Consistent with this, in addition to having a decreased amount of WAT, the $SRA^{-/-}$ mice also had reduced expression or a trend toward reduced expression of the adipocyte genes fatty acid-binding protein 4 (*Fabp4*), and adiponectin (*Adipoq*) in the sWAT (Fig. 3*G*) and eWAT (Fig. 3*F*). In contrast, $SRA^{-/-}$ mice had a trend toward increased eWAT expression of phosphoenolpyruvate carboxykinase 1 (*Pck1*), an enzyme that regulates the balance between free fatty acids and triglycerides in adipose tissue (Fig. 3*F*).

In addition, $SRA^{-/-}$ mice had reduced eWAT expression of the inflammation genes tumor necrosis factor α (*Tnf*) and chemokine (C-C motif) ligand 2 (*Ccl2*) (also known as MCP-1), and a trend to reduced interleukin 6 (*Il6*) (Fig. 3*F*). This is important because diet-induced obesity is known to be a state of increased inflammation (30). Steroid nuclear receptor coactivators (SRCs), which include *Ncoa1* (SRC1), *Ncoa2* (SRC2), and *Ncoa3* (SRC3), are implicated in the control metabolism. $SRC1^{-/-}$ mice are prone to, but $SRC2^{-/-}$ and $SRC\text{-}3^{-/-}$ are protected against, diet-induced obesity (31, 32). As shown in Fig. 3*F*, the expression of all three SRC genes is unchanged in the $SRA^{-/-}$ mice, suggesting that expression of these genes is neither dependent on SRA nor altered in an attempt to compensate for the loss of SRA.

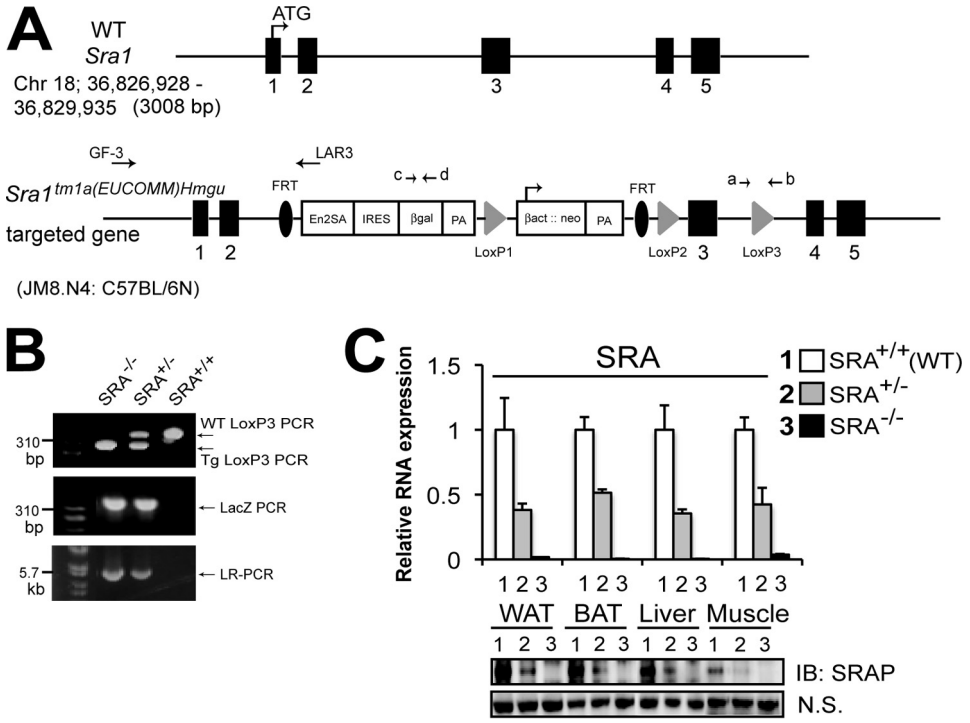

FIGURE 2. **Generation and validation of SRAKO.** *A*, strategy of *Sra1* gene targeting of the mouse genome to produce the *Sra1*$^{tm1a(EUCOMM)Hmgu}$ knock-out allele (*SRA*$^{-}$). PCR primer locations used for genotyping are shown schematically. *B*, genotyping SRA$^{+/+}$, SRA$^{+/-}$, and SRA$^{-/-}$ mice by PCR using primers shown schematically above. Primers *a* and *b* span the LoxP3 site (Lox P3 PCR), *c* and *d* span the *lacZ* site (*lacZ* PCR), and *GF3* and *LAR3* span the *Sra1* gene 5′ genomic DNA and target vector by long range PCR. Note that primers *a* and *b* of the PCR product are larger for WT than for the targeted allele, because the construct has a 119-bp deletion internal to the primer sites. *C*, *upper panel*, validation of SRA global KO by RT-qPCR, data were normalized to *Ppia* mRNA and expressed relative to the level in SRA$^{+/+}$, $n = 4$ mice at age of 8 weeks; *lower panel*, SRAP content determined by immunoblot (*IB*) in WAT, BAT, liver, and muscle; *N.S.*, nonspecific band used as a loading control in the same blot with anti-SRAP.

In addition to the classical and constitutive BAT located in the interscapular region of mice, recent studies have revealed a recruitable BAT that resides within WAT, which has alternatively been called beige, brite, or inducible BAT (33–36). Beige adipocytes are most abundant in the inguinal WAT, a major subcutaneous fat depot in rodents (37). Brown and beige adipocytes express high levels of *Ucp1* and other thermogenic genes (34, 36), and therefore have the potential to counteract obesity and type 2 diabetes. Because increased activities of brown and beige adipocytes have been linked to obesity resistance in many mouse models (38), we assessed the expression of beige adipocyte genes in the sWAT of SRA$^{-/-}$ mice under HFD feeding. Overall, we did not find strong evidence of sWAT browning. The sWAT of SRA$^{-/-}$ mice showed decreased expression of the brown adipocyte marker PR domain-containing protein 16 (*Prdm16*), and no change in the expression of *Ucp1* or *CD137*, a beige adipocyte cell surface marker (36) (Fig. 3*G*). However, SRA$^{-/-}$ mice under HFD feeding did have increased sWAT expression of *Fndc5* (Irisin), which has recently been shown to stimulate *Ucp-1* expression in white adipocytes in culture and increase energy expenditure in mice (39). In addition, there was a trend of increased expression of *Bmp8b*, which has the capacity to increase energy dissipation in BAT (40), and of the beige adipocyte marker *Tbx1* (36, 41), but not of *Tbx15*.

Furthermore, SRA$^{-/-}$ mice also had reduced interscapular BAT mass with reduced brown adipocyte size (Fig. 4, *A* and *B*). The expression levels of several BAT genes within the SRA$^{-/-}$ BAT were similar to those in WT mice (Fig. 4*C*).

Energy Expenditure Is Unchanged in SRA$^{-/-}$ *Mice*—Because adiposity is determined by the balance of calorie intake and utilization, we investigated parameters of energy homeostasis in SRA$^{-/-}$ and WT control mice. In considering the contributions of both LBM and fat mass (FM), we normalized oxygen consumption and carbon dioxide production to LBM plus 20% FM (LBM + 0.2FM), as this has been shown to be a more accurate way to account for variations in FM than simple normalization to LBM or total body weight (27). Upon this analysis, oxygen consumption and respiratory quotient were not significantly changed in SRA$^{-/-}$ mice (Fig. 5, *A* and *B*). Furthermore, the absolute food intake of SRA$^{-/-}$ mice from a 42-day average was unaltered on a normal chow diet (data not shown) and during HFD feeding (Fig. 5, *A* and *B*). In addition, the total locomotor activity was also unchanged between the two groups (Fig. 5, *A* and *B*) during HFD feeding. These experiments suggest that the lean phenotype of SRA$^{-/-}$ mice does not result from changes of caloric intake and energy expenditure. However, as will be discussed below, it is possible that changes in these parameters were too subtle to detect.

SRA$^{-/-}$ *Mice Have Improved Insulin Sensitivity and Decreased Liver Fat*—Consistent with the reduced fat mass with HFD feeding, SRA$^{-/-}$ mice had significantly reduced insulin levels with no change in fasting blood glucose compared with the WT control mice (Fig. 6*A*). In addition, there was a trend toward lower plasma leptin, and no change in plasma adiponectin, TG, or free fatty acid levels. Furthermore, HFD-fed SRA$^{-/-}$ mice had improved glucose tolerance following intraperitoneal glucose challenge relative to HFD-fed WT mice (Fig. 6*B*), as well as

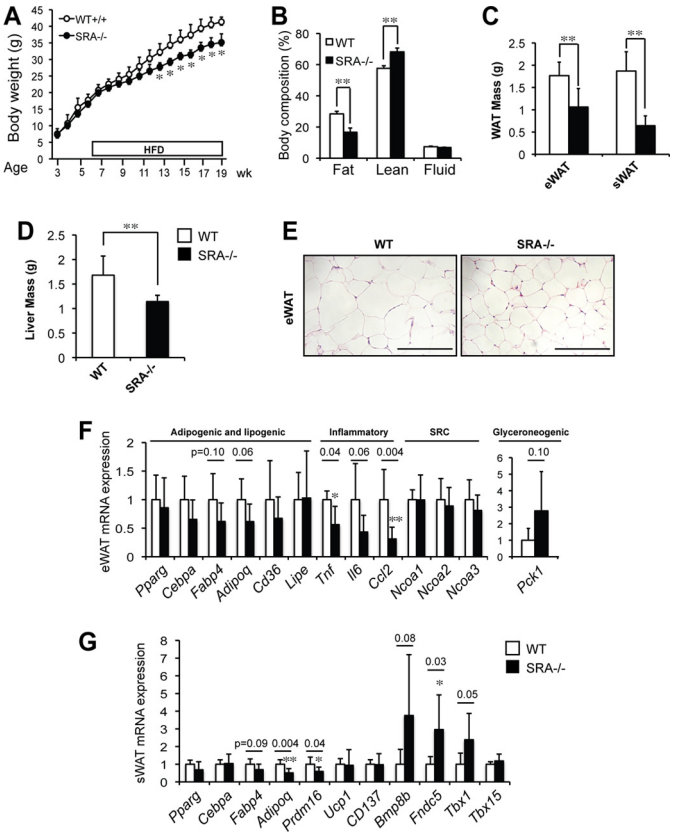

FIGURE 3. **SRAKO protects from diet-induced obesity and inhibits adipogenic, lipogenic, and inflammatory gene expression in WAT.** *A*, SRAKO inhibits HFD-induced obesity (*DIO*). Male mice body weights were measured from 3 to 19 weeks of age. HFD was started at 6 weeks of age. $SRA^{+/+}$, $n = 6$, and $SRA^{-/-}$, $n = 7$. *B*, body composition was determined by nuclear magnetic resonance after DIO. *C* and *D*, reduced eWAT, sWAT, and liver mass in $SRA^{-/-}$ mice after DIO. *E*, histology of eWAT in H&E-stained sections. *Scale bar*, 200 μm. *F*, RT-qPCR analysis of mRNA expression in eWAT at the end of DIO. *G*, RT-qPCR analysis of mRNA expression in subcutaneous WAT at the end of DIO. *F* and *G*, data were normalized to 60 S ribosomal protein L10E (*Rplp0*) mRNA, *, $p < 0.05$ and **, $p < 0.01$, $n = 6–7$. *SRC*, steroid receptor coactivators.

more marked hypoglycemia following insulin challenge (Fig. 6*C*). Consistent with this increased insulin sensitivity, HFD-fed $SRA^{-/-}$ mice had increased Akt phosphorylation in WAT, liver, and gastrocnemius muscle following insulin challenge, relative to HFD-fed WT mice (Fig. 6*D*).

The proinflammatory cytokine TNFα is produced in adipose tissue and is elevated in obesity and correlates with insulin resistance (42). $SRA^{-/-}$ mice had reduced plasma TNFα levels, but unchanged levels of IL6, another inflammatory cytokine correlated with insulin resistance (43) (Fig. 6*E*).

In humans, as a hallmark of the metabolic syndrome, fatty liver is tightly associated with insulin resistance and type 2 diabetes (44). SRA is well expressed in the liver (Fig. 1). Interestingly, $SRA^{-/-}$ mice had a 30% reduction in liver weight compared with WT controls after HFD feeding (Fig. 3*D*). Strikingly, in contrast to the large lipid droplets that were apparent by H&E staining in the livers from WT mice, lipid droplets were greatly reduced in the livers of $SRA^{-/-}$ mice (Fig. 7*A*). Further investigation revealed that liver triglyceride and free fatty acid levels were 61 and 54% lower in $SRA^{-/-}$ mice than WT controls with HFD feeding, respectively (Fig. 7, *B* and *C*). To further investigate this protection from hepatosteatosis, we analyzed the expression of key lipogenic and metabolic genes in the livers of HFD-fed $SRA^{-/-}$ and WT mice. As shown in Fig. 7*D*, the expression of *Ppara*, *Pparg*, *Fabp4*, and hormone-sensitive lipase (*Lipe*) was significantly reduced in the livers of $SRA^{-/-}$ mice, with a trend toward reduced expression of stearoyl-coenzyme A desaturase 1 (*Scd1*) ($p = 0.051$). These data suggest that the decreased fatty liver in $SRA^{-/-}$ mice may contribute to the improved insulin sensitivity. However, the expression of several genes involved in hepatic gluconeogenesis and glycolysis was not significantly changed.

DISCUSSION

We have previously shown that overexpression of the lncRNA SRA in ST2 mesenchymal precursor cells promotes their differentiation into adipocytes, and that knockdown of endogenous SRA inhibits 3T3-L1 cell differentiation into adipocytes (26). Here we demonstrate an important role for SRA in adipocyte biology in mice *in vivo*. To our knowledge, this is the first report for a lncRNA playing a role in the regulation of fat mass *in vivo*. We found that SRA is expressed at a much higher level in adipose tissue than other mouse organs. Also, SRA is induced in WAT in mice under HFD feeding. Global knock-out of SRA protects against diet-induced obesity and improves whole body glucose homeostasis. These results are consistent with *in vitro* data showing that SRA can function as a PPARγ coactivator. We cannot rule out the potential coactivation by SRA of other transcription factors that may play roles in adipogenesis. For example, SRA can promote glucocorticoid receptor-mediated transactivation (14), and recently the glucocorticoid receptor has been shown to play an important role regulating early adipogenesis (7). In addition, our microarray data reveal hundreds of SRA-responsive genes in adipocyte cell lines in culture, including genes related to cell cycle, insulin, and TNFα signaling (26). Although many of these SRA-mediated changes are likely indirect, a substantial fraction may be direct given that SRA is a transcriptional coregulator. Thus, the contribution of SRA to adipogenesis *in vivo* may be complex and through multiple pathways.

The mechanism of transcriptional coactivation by SRA is not resolved, but SRA exists in a ribonucleoprotein complex and may serve as a scaffold to recruit coactivator proteins to target genes. In addition, lncRNAs can bind to DNA to form a RNA:DNA:DNA triplex (45), which has been proposed to recruit lncRNA-binding proteins to DNA (46).

The *Sra1* gene is unusual in that it expresses both a lncRNA (SRA) and a protein (SRAP) by alternative splicing (18, 19). Based upon cell culture experiments with the non-coding SRA RNA (26), it is most likely that this lncRNA exerts the major adipogenic effects observed here. However, because the mouse knock-out abolishes expression of both SRA and SRAP, we cannot exclude a possible role of SRAP in adipocytes.

$SRA^{-/-}$ mice under HFD feeding demonstrate reduced adiposity with decreased percent of body fat and increased percent of lean mass (Fig. 3). This observation is further evidenced by reduced epididymal and subcutaneous WAT mass, reduced BAT mass, and decreased expression of several WAT marker genes (Fig. 3). Recent studies indicate that "brown-like" cells exist in subcutaneous WAT, called beige cells or brite cells (34, 36, 47, 48). The activities of both classical brown and beige fat

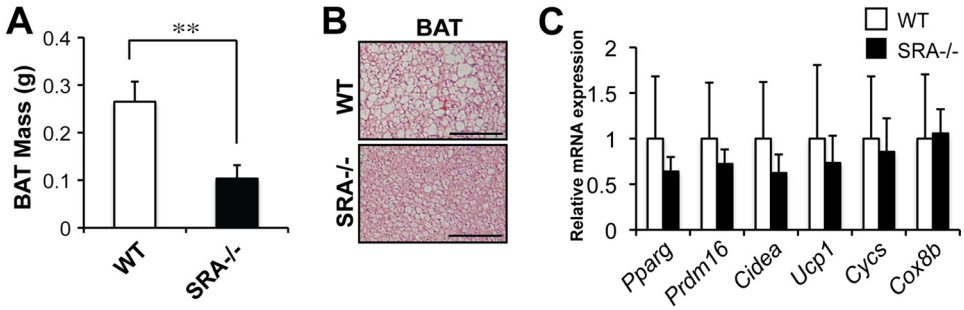

FIGURE 4. **SRAKO reduces brown fat mass and results in smaller brown adipocytes.** *A*, SRAKO reduced interscapular BAT mass after DIO. *B*, histology of BAT in H&E-stained sections. *Scale bar*, 200 μm. *C*, brown adipocyte mRNA expression was determined by RT-qPCR. Data were normalized to *Rplp0* mRNA, $n = 6–7$.

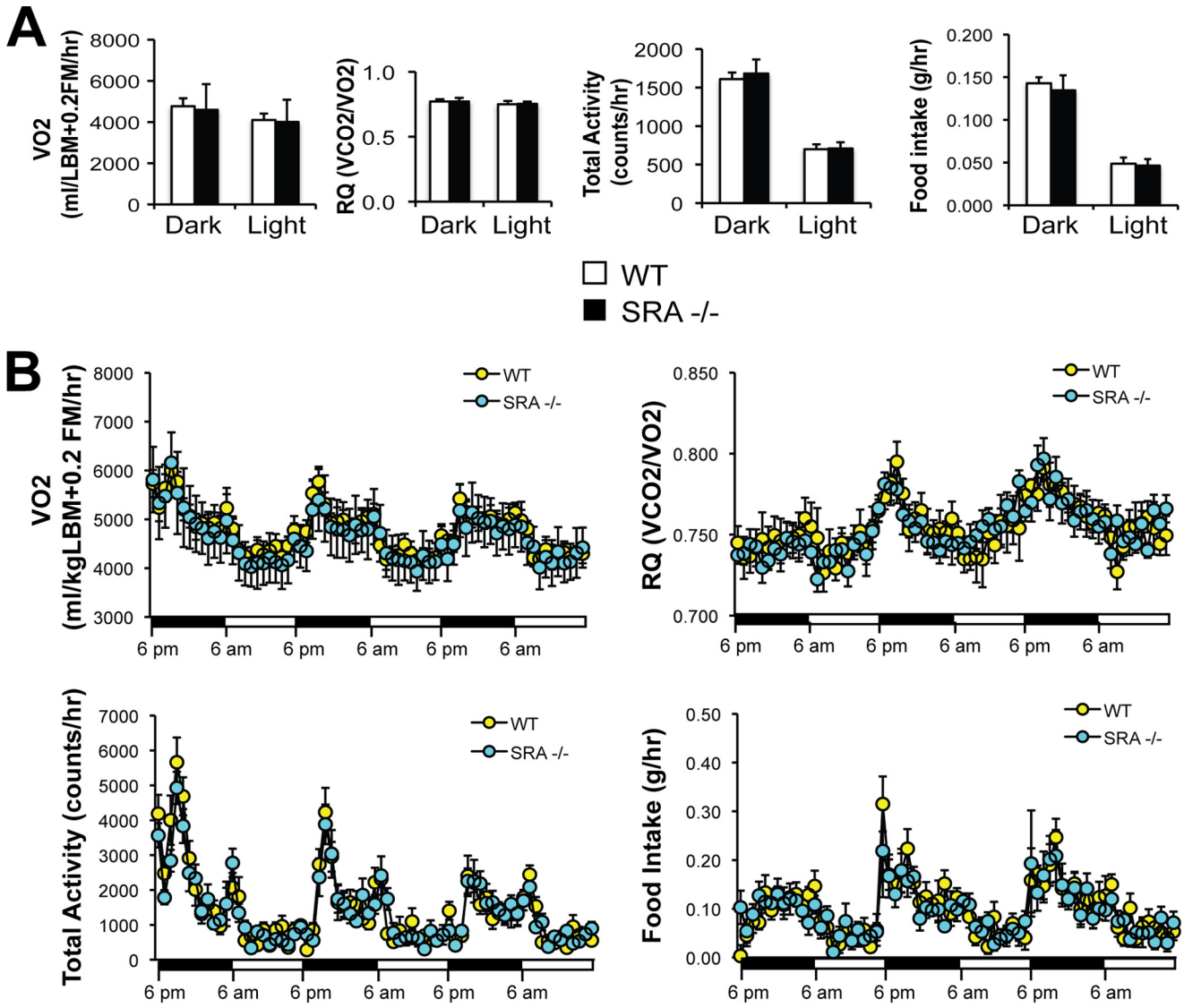

FIGURE 5. **Energy expenditure profile in WT and SRA$^{-/-}$ mice upon DIO.** Oxygen consumption, respiratory quotient (*RQ*), total activity, and food intake were determined over 3 days in SRA$^{-/-}$ and WT mice at the end of 14 weeks of HFD feeding, $n = 6–7$ mice per group. The data in *panel A* represent the average dark and light cycle measurements during the third measurement day. The data in *panel B* represent the profiles across all 3 days.

cells reduce obesity in mice and correlate with leanness in human (38, 49). However, SRA$^{-/-}$ mice did not have a generalized increase in beige cell markers within WAT at the end of the HFD feeding. Overall, these data suggest that the reduced adiposity in these mice is not due to increased activity of BAT and beige fat cells.

Our data indicate that SRAKO in mice improves whole body insulin sensitivity when fed a HFD (Fig. 6, *B* and *C*). This effect also is manifest at a molecular level, because the SRA$^{-/-}$ mice show increased phosphorylation of Akt in WAT, liver, and muscle in response to acute insulin challenge (Fig. 6*D*). Because these mice have decreased fat mass, the simplest explanation

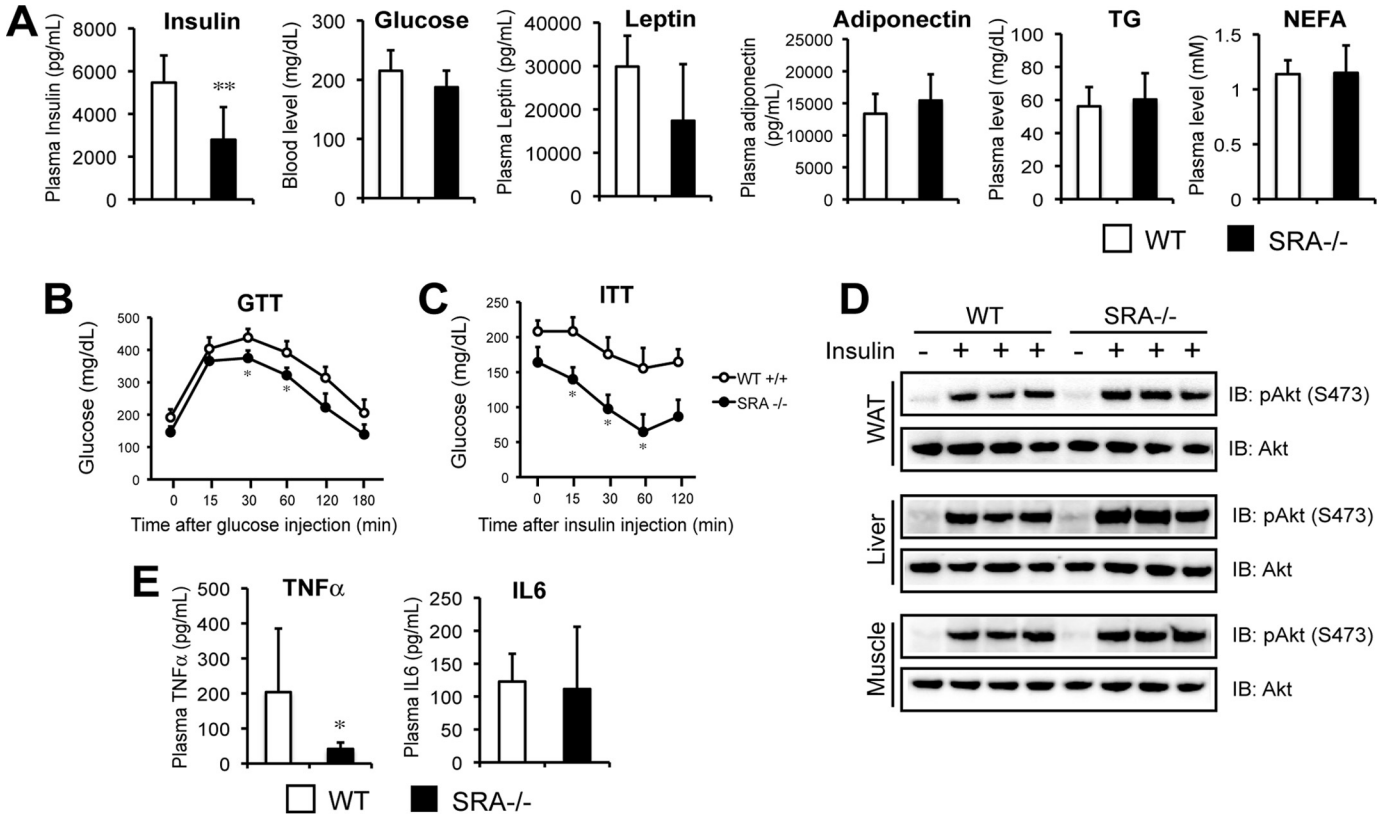

FIGURE 6. **SRAKO improves DIO-induced insulin resistance.** *A*, plasma hormone levels in SRA$^{-/-}$ mice were analyzed and compared with WT controls. All data in this figure were measured at the end of DIO. Blood glucose, plasma TG, and free fatty acid (non-esterified fatty acid) levels were measured at fasting conditions (6 h), $n = 6–7$. *B*, glucose tolerance test (*GTT*) at the end of DIO. Mice were fasted overnight (16 h), and a standard glucose tolerance test was performed. *C*, insulin tolerance test (*ITT*) at the end point of DIO. Mice were fasted for 6 h during the day, and a standard insulin tolerance test was performed, $n = 6–7$ mice. *D*, SRAKO enhances insulin-stimulated phosphorylation of Akt under HFD feeding. HFD-fed SRA$^{-/-}$ and WT control mice were fasted overnight (16 h). Five minutes after PBS or insulin injection via tail vein, epididymal WAT, liver, and gastrocnemius muscles were dissected. The tissue lysates were immunoblotted for pAkt (Ser-473) and total Akt. *E*, plasma TNFα and IL6 levels were analyzed as described for *panel A*. *, $p < 0.05$; **, $p < 0.01$; *IB*, immunoblot.

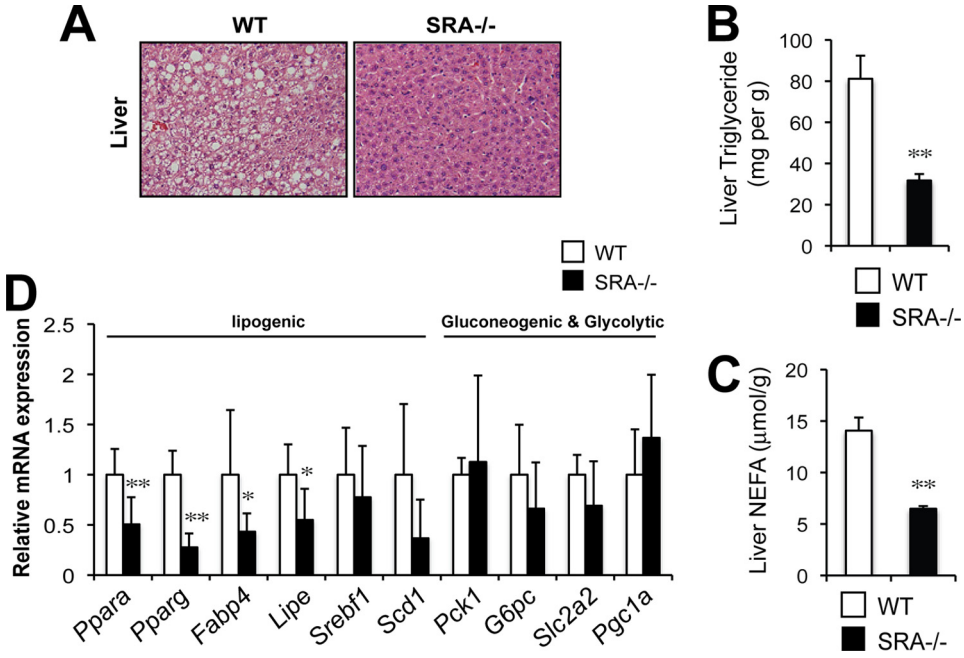

FIGURE 7. **SRAKO inhibits the formation of fatty liver under HFD.** *A*, H&E sections of liver at the end point of DIO. *B* and *C*, liver TG and non-esterified fatty acid levels were analyzed, respectively, $n = 6–7$. *D*, RT-qPCR analysis of expression of liver genes involved in lipogenesis, gluconeogenesis, and glycolysis. Data were normalized to *Ppia* mRNA and relative to the expression of each gene in WT mice, $n = 6–7$. *, $p < 0.05$ and **, $p < 0.01$.

for the improved insulin sensitivity is a direct effect of loss of SRA on adipogenesis and adipocyte function, probably at least in part through decreased PPARγ function. However, these mice have a global loss of SRA, and therefore other tissues may contribute to improved whole body insulin sensitivity. For example, SRA is expressed at significant levels in liver, and SRAKO mice have decreased hepatic steatosis. Whether the loss of hepatocyte SRA is a factor in this remains to be determined.

Furthermore, it is well recognized that chronic tissue inflammation is an important cause of obesity-induced insulin resistance (3, 50). One example of evidence for this relationship is that the cytokine TNFα is elevated in the adipose tissue of obese rodents and inhibition of this cytokine improves glucose tolerance and insulin sensitivity (42). Importantly, compared with WT control mice, SRA$^{-/-}$ mice have significantly reduced expression of a subset of inflammation genes including *Tnf* (TNFα) and *Ccl2* (MCP-1) in WAT (Fig. 3*F*) and decreased plasma TNFα levels (Fig. 6*E*). These results suggest that reduced inflammatory signaling may contribute significantly to the improved insulin sensitivity in SRA$^{-/-}$ mice. Because SRA is expressed at a relatively high level in mouse spleen (Fig. 1), as well as in monocytes derived from mouse spleen and murine macrophage J774A.1 cells (data not shown), SRAKO may have direct anti-inflammatory effects on the immune system.

It is at first glance puzzling that SRA$^{-/-}$ mice are protected from diet-induced obesity, yet there is no detectable change in food intake or energy expenditure. Perhaps they are inefficient at absorbing food from the gut, which could be an effect of SRAKO in the mouse itself or a secondary effect on the gut microbiome (51, 52). It also is possible that changes in energy expenditure or food intake went undetected because they are too subtle. For example, it has been calculated that for mice to gain an excess of 10 g over 25 weeks (a rate of change almost identical to that observed in this study), an energy imbalance of only ~3% is required (27). Detecting a 2.5% change in energy intake with 80% power would require a sample size of 350 mice (53), and detecting the expected changes would be even more daunting if the underlying basis is multifactorial.

In summary, the current studies, which are the first report of an *in vivo* SRA knock-out, demonstrate an important role for SRA in the regulation of adipose tissue mass, fatty liver, glucose homeostasis, and metabolism-related gene expressions *in vivo*. Future studies using tissue-specific knockouts will help clarify the underlying mechanisms regarding whole animal insulin sensitivity and will shed further light on the biological functions of SRA as a potential target to control obesity and type 2 diabetes.

Acknowledgments—We thank Drs. Martin Myers and Liangyou Rui for helpful discussions. The mouse metabolic studies were performed by the University of Michigan Nutrition Obesity Research Center (P30DK089503).

REFERENCES

1. Gesta, S., Tseng, Y. H., and Kahn, C. R. (2007) Developmental origin of fat: tracking obesity to its source. *Cell* **131,** 242–256
2. Doria, A., Patti, M. E., and Kahn, C. R. (2008) The emerging genetic architecture of type 2 diabetes. *Cell Metab.* **8,** 186–200
3. Olefsky, J. M., and Glass, C. K. (2010) Macrophages, inflammation, and insulin resistance. *Annu. Rev. Physiol.* **72,** 219–246
4. Barak, Y., Nelson, M. C., Ong, E. S., Jones, Y. Z., Ruiz-Lozano, P., Chien, K. R., Koder, A., and Evans, R. M. (1999) PPARγ is required for placental, cardiac, and adipose tissue development. *Mol. Cell* **4,** 585–595
5. Farmer, S. R. (2006) Transcriptional control of adipocyte formation. *Cell Metab.* **4,** 263–273
6. Linhart, H. G., Ishimura-Oka, K., DeMayo, F., Kibe, T., Repka, D., Poindexter, B., Bick, R. J., and Darlington, G. J. (2001) C/EBPα is required for differentiation of white, but not brown, adipose tissue. *Proc. Natl. Acad. Sci. U.S.A.* **98,** 12532–12537
7. Siersbæk, R., Nielsen, R., John, S., Sung, M. H., Baek, S., Loft, A., Hager, G. L., and Mandrup, S. (2011) Extensive chromatin remodelling and establishment of transcription factor "hotspots" during early adipogenesis. *EMBO J.* **30,** 1459–1472
8. Steger, D. J., Grant, G. R., Schupp, M., Tomaru, T., Lefterova, M. I., Schug, J., Manduchi, E., Stoeckert, C. J., Jr., and Lazar, M. A. (2010) Propagation of adipogenic signals through an epigenomic transition state. *Genes Dev.* **24,** 1035–1044
9. Lowe, C. E., O'Rahilly, S., and Rochford, J. J. (2011) Adipogenesis at a glance. *J. Cell Sci.* **124,** 2681–2686
10. Cristancho, A. G., and Lazar, M. A. (2011) Forming functional fat: a growing understanding of adipocyte differentiation. *Nat. Rev. Mol. Cell Biol.* **12,** 722–734
11. Rosen, E. D., and MacDougald, O. A. (2006) Adipocyte differentiation from the inside out. *Nat. Rev. Mol. Cell Biol.* **7,** 885–896
12. Rinn, J. L., and Chang, H. Y. (2012) Genome regulation by long noncoding RNAs. *Annu. Rev. Biochem.* **81,** 145–166
13. Wang, X., Song, X., Glass, C. K., and Rosenfeld, M. G. (2011) The long arm of long noncoding RNAs: roles as sensors regulating gene transcriptional programs. *Cold Spring Harbor Perspect. Biol.* **3,** a003756
14. Lanz, R. B., McKenna, N. J., Onate, S. A., Albrecht, U., Wong, J., Tsai, S. Y., Tsai, M. J., and O'Malley, B. W. (1999) A steroid receptor coactivator, SRA, functions as an RNA and is present in an SRC-1 complex. *Cell* **97,** 17–27
15. Xu, B., and Koenig, R. J. (2004) An RNA-binding domain in the thyroid hormone receptor enhances transcriptional activation. *J. Biol. Chem.* **279,** 33051–33056
16. Zhao, X., Patton, J. R., Davis, S. L., Florence, B., Ames, S. J., and Spanjaard, R. A. (2004) Regulation of nuclear receptor activity by a pseudouridine synthase through posttranscriptional modification of steroid receptor RNA activator. *Mol. Cell* **15,** 549–558
17. Caretti, G., Schiltz, R. L., Dilworth, F. J., Di Padova, M., Zhao, P., Ogryzko, V., Fuller-Pace, F. V., Hoffman, E. P., Tapscott, S. J., and Sartorelli, V. (2006) The RNA helicases p68/p72 and the noncoding RNA SRA are coregulators of MyoD and skeletal muscle differentiation. *Dev. Cell* **11,** 547–560
18. Emberley, E., Huang, G. J., Hamedani, M. K., Czosnek, A., Ali, D., Grolla, A., Lu, B., Watson, P. H., Murphy, L. C., and Leygue, E. (2003) Identification of new human coding steroid receptor RNA activator isoforms. *Biochem. Biophys. Res. Commun.* **301,** 509–515
19. Kawashima, H., Takano, H., Sugita, S., Takahara, Y., Sugimura, K., and Nakatani, T. (2003) A novel steroid receptor co-activator protein (SRAP) as an alternative form of steroid receptor RNA-activator gene: expression in prostate cancer cells and enhancement of androgen receptor activity. *Biochem. J.* **369,** 163–171
20. Hubé, F., Velasco, G., Rollin, J., Furling, D., and Francastel, C. (2011) Steroid receptor RNA activator protein binds to and counteracts SRA RNA-mediated activation of MyoD and muscle differentiation. *Nucleic Acids Res.* **39,** 513–525
21. Xu, B., Yang, W. H., Gerin, I., Hu, C. D., Hammer, G. D., and Koenig, R. J. (2009) Dax-1 and steroid receptor RNA activator (SRA) function as transcriptional coactivators for steroidogenic factor 1 in steroidogenesis. *Mol. Cell. Biol.* **29,** 1719–1734
22. Lanz, R. B., Razani, B., Goldberg, A. D., and O'Malley, B. W. (2002) Distinct RNA motifs are important for coactivation of steroid hormone receptors by steroid receptor RNA activator (SRA). *Proc. Natl. Acad. Sci. U.S.A.* **99,**

16081–16086
23. Leygue, E., Dotzlaw, H., Watson, P. H., and Murphy, L. C. (1999) Expression of the steroid receptor RNA activator in human breast tumors. *Cancer Res.* **59,** 4190–4193
24. Murphy, L. C., Simon, S. L., Parkes, A., Leygue, E., Dotzlaw, H., Snell, L., Troup, S., Adeyinka, A., and Watson, P. H. (2000) Altered expression of estrogen receptor coregulators during human breast tumorigenesis. *Cancer Res.* **60,** 6266–6271
25. Friedrichs, F., Zugck, C., Rauch, G. J., Ivandic, B., Weichenhan, D., Müller-Bardorff, M., Meder, B., El Mokhtari, N. E., Regitz-Zagrosek, V., Hetzer, R., Schäfer, A., Schreiber, S., Chen, J., Neuhaus, I., Ji, R., Siemers, N. O., Frey, N., Rottbauer, W., Katus, H. A., and Stoll, M. (2009) HBEGF, SRA1, and IK: three cosegregating genes as determinants of cardiomyopathy. *Genome Res.* **19,** 395–403
26. Xu, B., Gerin, I., Miao, H., Vu-Phan, D., Johnson, C. N., Xu, R., Chen, X. W., Cawthorn, W. P., MacDougald, O. A., and Koenig, R. J. (2010) Multiple roles for the non-coding RNA SRA in regulation of adipogenesis and insulin sensitivity. *PLoS One* **5,** e14199
27. Even, P. C., and Nadkarni, N. A. (2012) Indirect calorimetry in laboratory mice and rats: principles, practical considerations, interpretation and perspectives. *Am. J. Physiol. Regul. Integr. Comp. Physiol.* **303,** R459–476
28. Du, B., Cawthorn, W. P., Su, A., Doucette, C. R., Yao, Y., Hemati, N., Kampert, S., McCoin, C., Broome, D. T., Rosen, C. J., Yang, G., and MacDougald, O. A. (2013) The transcription factor paired-related homeobox 1 (Prrx1) inhibits adipogenesis by activating transforming growth factor-β (TGFβ) signaling. *J. Biol. Chem.* **288,** 3036–3047
29. Skarnes, W. C., Rosen, B., West, A. P., Koutsourakis, M., Bushell, W., Iyer, V., Mujica, A. O., Thomas, M., Harrow, J., Cox, T., Jackson, D., Severin, J., Biggs, P., Fu, J., Nefedov, M., de Jong, P. J., Stewart, A. F., and Bradley, A. (2011) A conditional knockout resource for the genome-wide study of mouse gene function. *Nature* **474,** 337–342
30. Glass, C. K., and Olefsky, J. M. (2012) Inflammation and lipid signaling in the etiology of insulin resistance. *Cell Metab.* **15,** 635–645
31. Coste, A., Louet, J. F., Lagouge, M., Lerin, C., Antal, M. C., Meziane, H., Schoonjans, K., Puigserver, P., O'Malley, B. W., and Auwerx, J. (2008) The genetic ablation of SRC-3 protects against obesity and improves insulin sensitivity by reducing the acetylation of PGC-1α. *Proc. Natl. Acad. Sci. U.S.A.* **105,** 17187–17192
32. Picard, F., Géhin, M., Annicotte, J., Rocchi, S., Champy, M. F., O'Malley, B. W., Chambon, P., and Auwerx, J. (2002) SRC-1 and TIF2 control energy balance between white and brown adipose tissues. *Cell* **111,** 931–941
33. Guerra, C., Koza, R. A., Yamashita, H., Walsh, K., and Kozak, L. P. (1998) Emergence of brown adipocytes in white fat in mice is under genetic control. Effects on body weight and adiposity. *J. Clin. Invest.* **102,** 412–420
34. Petrovic, N., Walden, T. B., Shabalina, I. G., Timmons, J. A., Cannon, B., and Nedergaard, J. (2010) Chronic peroxisome proliferator-activated receptor γ (PPARγ) activation of epididymally derived white adipocyte cultures reveals a population of thermogenically competent, UCP1-containing adipocytes molecularly distinct from classic brown adipocytes. *J. Biol. Chem.* **285,** 7153–7164
35. Schulz, T. J., Huang, T. L., Tran, T. T., Zhang, H., Townsend, K. L., Shadrach, J. L., Cerletti, M., McDougall, L. E., Giorgadze, N., Tchkonia, T., Schrier, D., Falb, D., Kirkland, J. L., Wagers, A. J., and Tseng, Y. H. (2011) Identification of inducible brown adipocyte progenitors residing in skeletal muscle and white fat. *Proc. Natl. Acad. Sci. U.S.A.* **108,** 143–148
36. Wu, J., Boström, P., Sparks, L. M., Ye, L., Choi, J. H., Giang, A. H., Khandekar, M., Virtanen, K. A., Nuutila, P., Schaart, G., Huang, K., Tu, H., van Marken Lichtenbelt, W. D., Hoeks, J., Enerbäck, S., Schrauwen, P., and Spiegelman, B. M. (2012) Beige adipocytes are a distinct type of thermogenic fat cell in mouse and human. *Cell* **150,** 366–376
37. Vitali, A., Murano, I., Zingaretti, M. C., Frontini, A., Ricquier, D., and Cinti, S. (2012) The adipose organ of obesity-prone C57BL/6J mice is composed of mixed white and brown adipocytes. *J. Lipid Res.* **53,** 619–629
38. Harms, M., and Seale, P. (2013) Brown and beige fat: development, function and therapeutic potential. *Nat. Med.* **19,** 1252–1263
39. Boström, P., Wu, J., Jedrychowski, M. P., Korde, A., Ye, L., Lo, J. C., Rasbach, K. A., Boström, E. A., Choi, J. H., Long, J. Z., Kajimura, S., Zingaretti, M. C., Vind, B. F., Tu, H., Cinti, S., Højlund, K., Gygi, S. P., and Spiegelman, B. M. (2012) A PGC1-α-dependent myokine that drives brown fat-like development of white fat and thermogenesis. *Nature* **481,** 463–468
40. Whittle, A. J., Carobbio, S., Martins, L., Slawik, M., Hondares, E., Vázquez, M. J., Morgan, D., Csikasz, R. I., Gallego, R., Rodriguez-Cuenca, S., Dale, M., Virtue, S., Villarroya, F., Cannon, B., Rahmouni, K., López, M., and Vidal-Puig, A. (2012) BMP8B increases brown adipose tissue thermogenesis through both central and peripheral actions. *Cell* **149,** 871–885
41. Gburcik, V., Cawthorn, W. P., Nedergaard, J., Timmons, J. A., and Cannon, B. (2012) An essential role for Tbx15 in the differentiation of brown and "brite" but not white adipocytes. *Am. J. Physiol. Endocrinol. Metab.* **303,** E1053–1060
42. Hotamisligil, G. S., Shargill, N. S., and Spiegelman, B. M. (1993) Adipose expression of tumor necrosis factor-α: direct role in obesity-linked insulin resistance. *Science* **259,** 87–91
43. Arner, P. (2005) Resistin: yet another adipokine tells us that men are not mice. *Diabetologia* **48,** 2203–2205
44. Seppälä-Lindroos, A., Vehkavaara, S., Häkkinen, A. M., Goto, T., Westerbacka, J., Sovijärvi, A., Halavaara, J., and Yki-Järvinen, H. (2002) Fat accumulation in the liver is associated with defects in insulin suppression of glucose production and serum free fatty acids independent of obesity in normal men. *J. Clin. Endocrinol. Metab.* **87,** 3023–3028
45. Schmitz, K. M., Mayer, C., Postepska, A., and Grummt, I. (2010) Interaction of noncoding RNA with the rDNA promoter mediates recruitment of DNMT3b and silencing of rRNA genes. *Genes Dev.* **24,** 2264–2269
46. Martianov, I., Ramadass, A., Serra Barros, A., Chow, N., and Akoulitchev, A. (2007) Repression of the human dihydrofolate reductase gene by a non-coding interfering transcript. *Nature* **445,** 666–670
47. Ishibashi, J., and Seale, P. (2010) Medicine: beige can be slimming. *Science* **328,** 1113–1114
48. Seale, P., Conroe, H. M., Estall, J., Kajimura, S., Frontini, A., Ishibashi, J., Cohen, P., Cinti, S., and Spiegelman, B. M. (2011) Prdm16 determines the thermogenic program of subcutaneous white adipose tissue in mice. *J. Clin. Invest.* **121,** 96–105
49. Cypess, A. M., White, A. P., Vernochet, C., Schulz, T. J., Xue, R., Sass, C. A., Huang, T. L., Roberts-Toler, C., Weiner, L. S., Sze, C., Chacko, A. T., Deschamps, L. N., Herder, L. M., Truchan, N., Glasgow, A. L., Holman, A. R., Gavrila, A., Hasselgren, P. O., Mori, M. A., Molla, M., and Tseng, Y. H. (2013) Anatomical localization, gene expression profiling and functional characterization of adult human neck brown fat. *Nat. Med.* **19,** 635–639
50. Lumeng, C. N., and Saltiel, A. R. (2011) Inflammatory links between obesity and metabolic disease. *J. Clin. Invest.* **121,** 2111–2117
51. Turnbaugh, P. J., Ley, R. E., Mahowald, M. A., Magrini, V., Mardis, E. R., and Gordon, J. I. (2006) An obesity-associated gut microbiome with increased capacity for energy harvest. *Nature* **444,** 1027–1031
52. Vijay-Kumar, M., Aitken, J. D., Carvalho, F. A., Cullender, T. C., Mwangi, S., Srinivasan, S., Sitaraman, S. V., Knight, R., Ley, R. E., and Gewirtz, A. T. (2010) Metabolic syndrome and altered gut microbiota in mice lacking Toll-like receptor 5. *Science* **328,** 228–231
53. Tschöp, M. H., Speakman, J. R., Arch, J. R., Auwerx, J., Brüning, J. C., Chan, L., Eckel, R. H., Farese, R. V., Jr., Galgani, J. E., Hambly, C., Herman, M. A., Horvath, T. L., Kahn, B. B., Kozma, S. C., Maratos-Flier, E., Müller, T. D., Münzberg, H., Pfluger, P. T., Plum, L., Reitman, M. L., Rahmouni, K., Shulman, G. I., Thomas, G., Kahn, C. R., and Ravussin, E. (2012) A guide to analysis of mouse energy metabolism. *Nat. Methods* **9,** 57–63